

This is the online version of the paper in Proceedings Bridges 2007.

## Does it Look Square?

# Hexagonal Bipyramids, Triangular Antiprismoids, and their Fractals

Hideki Tsuiki

Graduate School of Human and Environmental Studies

Kyoto University

Yoshida-Nihonmatsu, Kyoto 606-8501, Japan

E-mail: tsuiki@i.h.kyoto-u.ac.jp

### Abstract

The Sierpinski tetrahedron is two-dimensional with respect to fractal dimensions though it is realized in three-dimensional space, and it has square projections in three orthogonal directions. We study its generalizations and present two-dimensional fractals with many square projections. One is generated from a hexagonal bipyramid which has square projections not in three but in **six** directions. Another one is generated from an octahedron which we call a triangular antiprismoid. These two polyhedra form a tiling of three-dimensional space, which is a Voronoi tessellation of three-dimensional space with respect to the union of two cubic lattices. We also present other fractals and show a simple object with three square projections obtained as the limit of such fractals.

### Sierpinski Tetrahedron and its Projections

Three-dimensional objects are interesting in that they change their appearances according to the way they are looked at and their shadow images change smoothly as they are rotated three-dimensionally. For some fractals in three-dimensional space, their shadow images are complicated fractal figures in many directions but sometimes they become simple shapes like the square, and they are really attractive.

For example, Sierpinski's tetrahedron is a popular fractal realized in three-dimensional space. It is self-similar in that it is equal to the union of four half-sized copies of itself. In fractal geometry, we say that an object has similarity dimension  $n$  when it is equal to the union of  $k^n$  copies of itself with  $1/k$  scale. Therefore, the Sierpinski tetrahedron is two dimensional with respects to the similarity dimension. We refer the reader to [1] and [2] for the theory of fractals. Figure 1 shows some of the shadow images of the Sierpinski tetrahedron. As Figure 1(b) shows, it has a solid square shadow image when projected from an edge. Since it has three pairs of edges opposite to each other, a Sierpinski tetrahedron has square shadow images when it is projected from three directions which are orthogonal to each other. Here, we count opposite directions once. It is true both for the mathematically-defined pure Sierpinski tetrahedron and for its  $n$ -th level approximation, which is composed of  $4^n$  regular tetrahedrons.

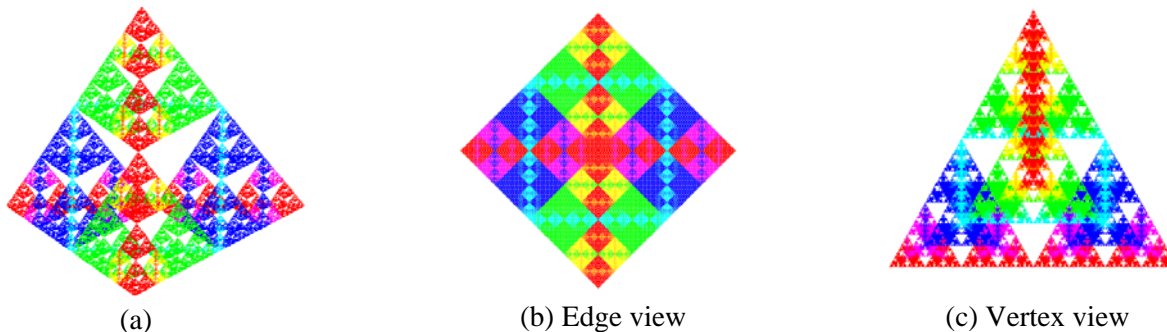


**Figure 1:** Some projection images of the Sierpinski Tetrahedron.

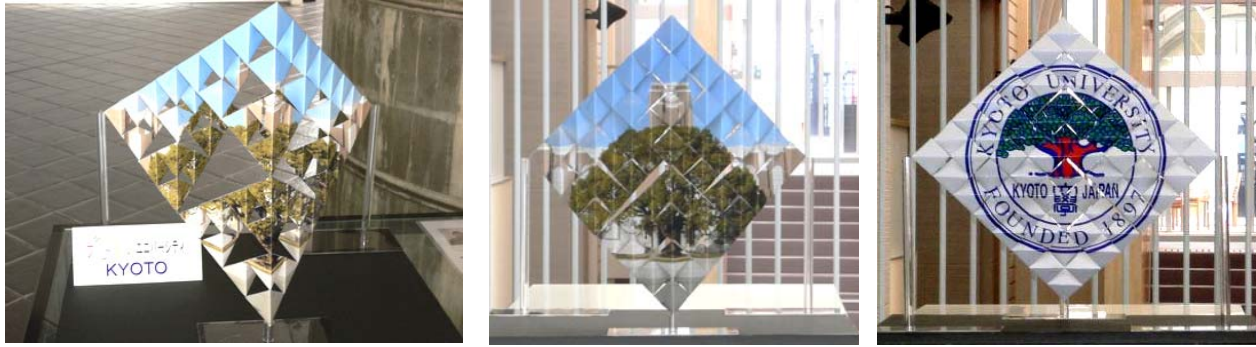


**Figure 2:** *Fractal University KYOTO (Polyurethane tetrahedron pieces connected by wires).*

The sculpture in Figure 2 is an application of this property. It has the shape of the 3rd level approximation of the Sierpinski tetrahedron, and two square pictures extended with the rate  $1 : \sqrt{3}$  are cut into  $4^n$  pieces and the pieces are pasted on two faces of the  $4^n$  tetrahedrons. We can view one picture from an edge, and the other one from the opposite side.

### Generalization of the Sierpinski Tetrahedron

Now, we consider other fractals in three-dimensional space with the same properties as the Sierpinski tetrahedron. For each  $k \geq 2$ , we consider self-similar fractals which satisfy the followings,

- (1) it is the union of  $k^2$  copies of itself with  $1/k$  scale,
- (2) it has square projections from three orthogonal directions, just as a cube has,
- (3) the similarity functions do not include rotational parts.

From property (1), the fractal has the similarity dimension two, and from property (3), the  $k^2$  copies have the same orientation as itself. Property (3) also ensures that the projection images are also self-similar, because each projection image is the union of the projection images of its small copies which are similar to the projection image of the whole because they have the same orientation. The theory of fractal geometry says that a fractal is determined only by the similarity functions, and for our case, they are again determined by their centers (i.e. the fixed points), because they do not include rotational parts and the scale is fixed to  $1/k$ . For the case of the Sierpinski tetrahedron,  $k$  is equal to 2 and the centers are the four vertices of the tetrahedron. The theory also says that, starting with any three-dimensional object containing the fractal, successive application of the IFS (i.e., the union of the similarity functions) will decrease its size and converges to the fractal. For the Sierpinski tetrahedron, we normally start with a tetrahedron to obtain a series of its approximations. However, condition (2) says that there is a cube with the same three projection images and this cubic approximation will make the structure of such a fractal very clear. Figure 3 shows the first three cubic approximations of the Sierpinski tetrahedron.

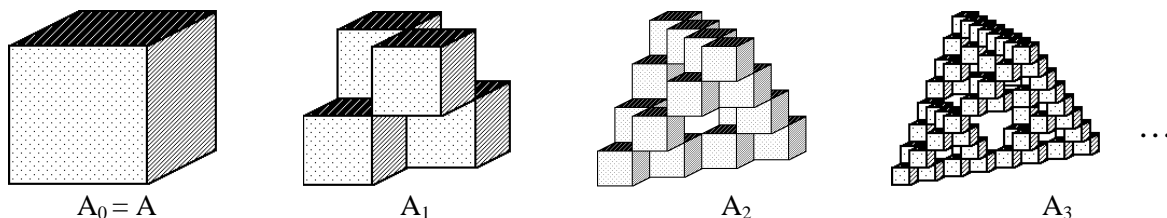


**Figure 3:** *Cubic approximations of the Sierpinski tetrahedron.*

Notice that the first approximation  $A_1$  consists of four cubes which are selected from the 8 cubes obtained by dividing the cube  $A$  into  $2 \times 2 \times 2$  and the four cubes are not overlapping when viewed from all the

three surface-directions of  $A$ . Since  $A_2, A_3, \dots$  are obtained by repeating this procedure, this fact ensures that each level of the approximation has three square projections. The Sierpinski tetrahedron is obtained as the intersection  $\bigcap_{i=1}^{\infty} A_i$  of these approximations, and it also has the same square projection for the following reason. Suppose that  $p$  is a point of this square and  $B_i \subset A_i$  its preimage by the projection from  $A_i$ . Each  $B_i$  is a closed set, and  $B_i \supset B_j$  when  $i < j$ . Therefore, their intersection  $C = \bigcap_{i=1}^{\infty} B_i$  is a non-empty set contained in the fractal and every point in  $C$  is projected to the point  $p$ .

We can generalize this procedure to every  $k$ . That is, dividing the cube  $A$  into  $k \times k \times k$  small cubes and selecting  $k^2$  of them so that they are not overlapping when viewed from the three surface directions. Each selection of such  $k^2$  cubes determines the similarity functions and thus a fractal object with three square projections. On the other hand, when a fractal satisfies properties (1) to (3), there exists a cube determined by the three projections in (2), and there are  $k^2$  cubes obtained by applying the similarity maps to this cube. Since their union contains the fractal, it must also have the square projection in three directions from (2). Therefore, every fractal with the properties (1) to (3) is obtained in this way.

When  $k = 2$ ,  $A_1$  is the only possible configuration if we identify those congruent through the rotation of the cube, and the Sierpinski tetrahedron is the only fractal with properties (1) to (3). When  $k = 3$ , we have two (non-congruent) ways of selecting 9 cubes from the 27 cubes, which are F and G in Figure 4. In the following two sections, we study those fractals generated by F and G.

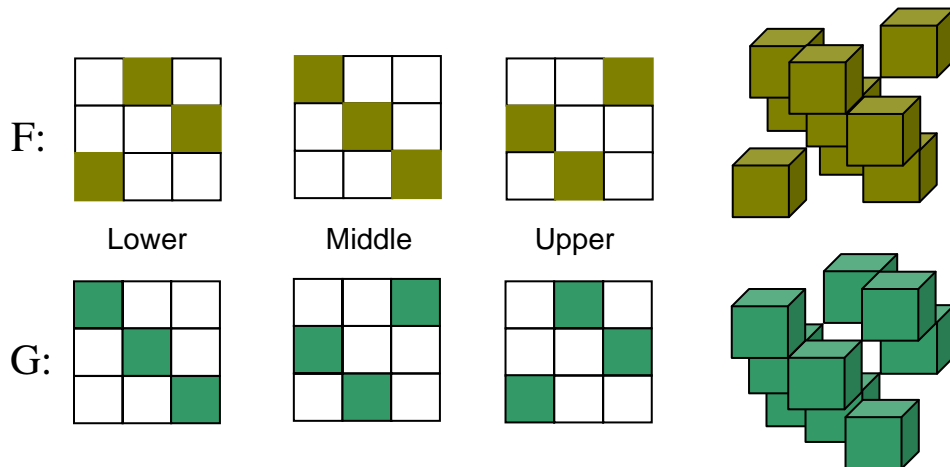
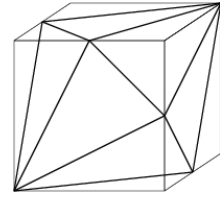
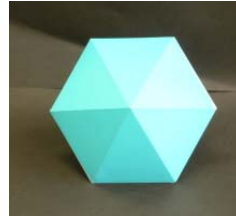


**Figure 4:** Two non-overlapping configurations of nine small cubes.

### The Hexagonal Bipyramid Fractal

In the lower part of Figure 5 are computer graphics images of the fractal generated by F viewed from many directions. This fractal has 6-fold symmetry. Because of this symmetry, it has square projections (Figure 5 (a)) not in three but in **six** directions. It also has two kinds of “dendrites” (b, e), two kinds of “snowflakes” (c, f), and two kinds of tiling patterns (d, g) which we will investigate later. Note that these projection images are self-similar, as we have noted in the previous section.

As we normally start not with a cube but with a regular tetrahedron to obtain a Sierpinski tetrahedron, it is more natural to start with the convex hull of the fractal to obtain its finite approximations. Since the similarity functions do not include rotation, the convex hull coincides with the convex hull of the centers of the similarity functions, which are (1) two vertices, (2) six middle points of edges, and (3) the center of the cube. As the result, we have a hexagonal bipyramid shown in the top of Figure 5. This dodecahedron



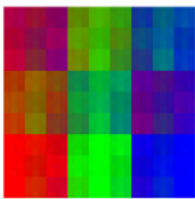
Hexagonal Bipyramid.



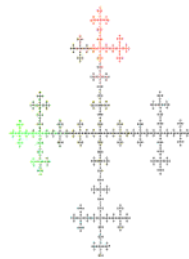
1<sup>st</sup> level approximation of the Hexagonal Bipyramid Fractal.



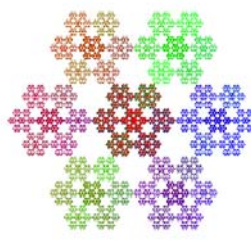
2<sup>nd</sup> level approximation with a SUDOKU coloring.



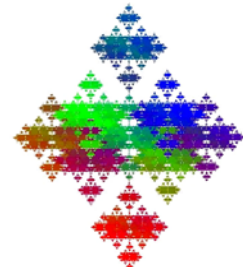
(a) Square (6)



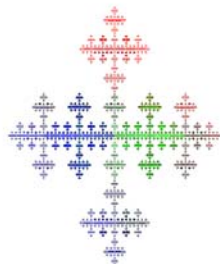
(b) Dendrite #1 (3)



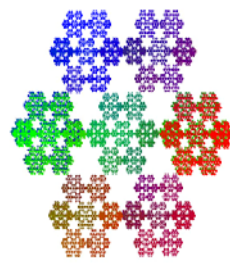
(c) Snowflake #1 (1)



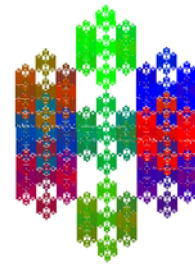
(d) Tiling #1 (6)



(e) Dendrite #2 (3)

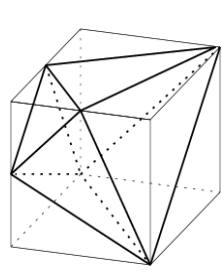


(f) Snowflake #2 (6)

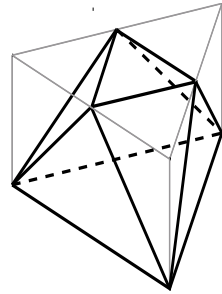


(g) Tiling #2 (6)

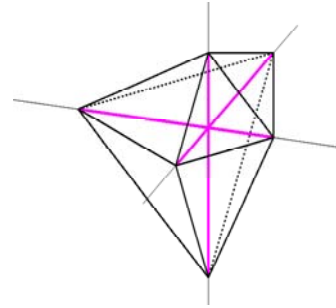
**Figure 5:** The hexagonal bipyramid fractal and its finite approximation models viewed from many directions. In the parenthesis are the numbers of directions in which we have such projection images (opposite directions counted once).



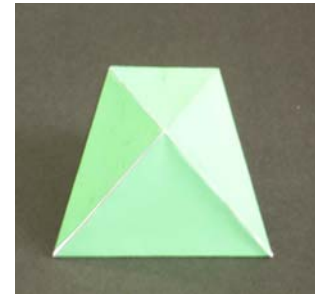
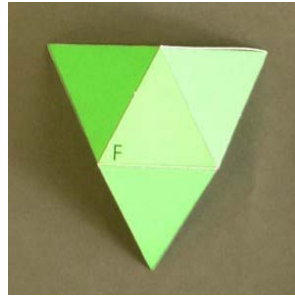
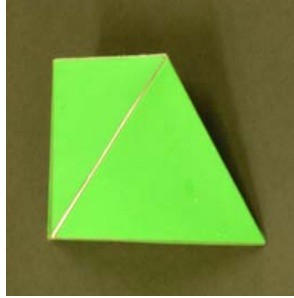
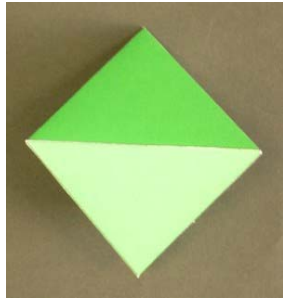
(a)



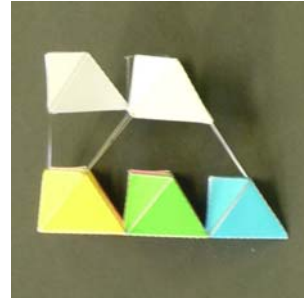
(b)



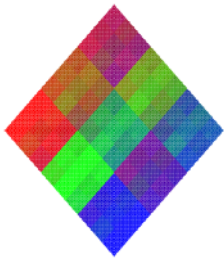
(c)



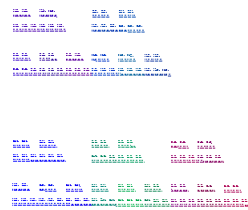
. Triangular Antiprismoid



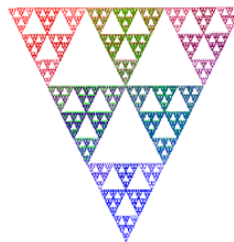
1<sup>st</sup> level approximation of the Triangular Antiprismoid Fractal.



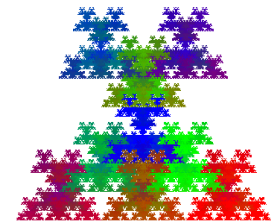
(d) Square (3)



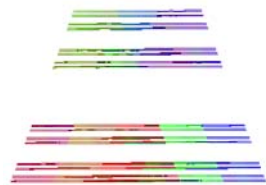
(e) Cantor Set #1 (3)



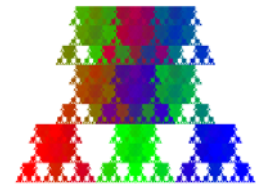
(f) Triangle (1)



(g) Tiling #1 (3)



(h) Cantor Set #2 (3)



(i) Tiling #2 (3)

**Figure 6:** The triangular antiprismoida fractal and its finite approximation models.

is the intersection of two cubes which share a diagonal, and each of its face is an isosceles triangle whose height is  $3/2$  of the base. As the upper-left picture shows, this hexagonal bipyramid is itself a polyhedron which has six square projections. Since the fractal generated from the configuration F is based on a hexagonal bipyramid, we will call it the hexagonal bipyramid fractal. We assembled level one and level two approximation models of the hexagonal bipyramid fractal with papers and piano wires (the second and the third row of Figure 5). This level two approximation model is colored with nine colors so that every nine rows and nine columns and nine blocks contain all the nine colors in each of the twelve square appearances. We will call it a SUDOKU coloring. It is calculated with a computer program that it has 30 SUDOKU colorings.

### The Triangular Antiprismoid Fractal

Figure 6 is about the fractal generated by the configuration G. In the lower part, there are figures of this fractal viewed from some directions. As property (2) says, this fractal has square projection images in three orthogonal directions (Figure (d)). As (e) and (h) show, this fractal is not connected. It is composed of slices which form the Cantor set. Figures (g) and (i) are fractal tiling images.

The convex hull of this fractal is obtained by taking the convex hull of the centers of the similarity maps, which are (1) three vertices, (2) three midpoints of edges, and (3) three center-points of faces of the cube. Here, the points in (3) are the middle points of the edges of the triangle generated from the points in (1), and thus can be omitted in taking the convex hull. Therefore, it has the form in Figure 6(a). This octahedron has square projections in three orthogonal directions. The two pictures of the square shape on the top left are taken from the opposite directions. Figure 6(b) shows another explanation of this octahedron, that is, it is a prismaoid obtained from a triangular prism by truncating three vertices of a base so that the new base becomes a triangle. We will call such a truncated prism an antiprismoid. Figure 9(c) shows yet another property of this triangular antiprismoid. That is, the six vertices are on the positive and the negative parts of the three axes of coordinates and the distance of the vertices from the origin on the negative parts is twice those on the positive parts.

### The $k \geq 4$ Case

The author wrote a program in Java to produce all the non-congruent configurations for the case  $k \leq 5$ . When  $k=4$ , there are 36 non-congruent fractals including the Sierpinski tetrahedron which already appeared for  $k=2$ . One of them is shown in Figure 7, which is the only connected one except for the Sierpinski tetrahedron. This fractal is also obtained through the IFS of 4 similarity maps with scale  $1/2$  and 180 degree rotation. Its convex hull is a non-Archimedean cuboctahedron with four of the triangular faces twice the size of the other four triangular faces. When  $k$  is equal to 5, we have 3482 fractals. There is a Java applet in the author's homepage which displays all the fractals up to  $k \leq 5$  [3].

As the number  $k$  increases, the number of two-dimensional fractals obtained in this way increases explosively. Among them, there is a series of fractals. Recall the configuration for the antiprismoid fractal in Figure 4(G). The lower level is a diagonal sequence of cubes, and the middle level is its shift to the right with the overflowed one appearing from the left. This construction of a configuration applies to every  $k$ , as the following figure shows.

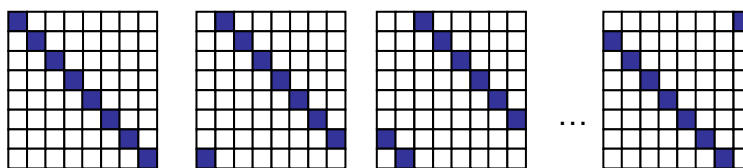
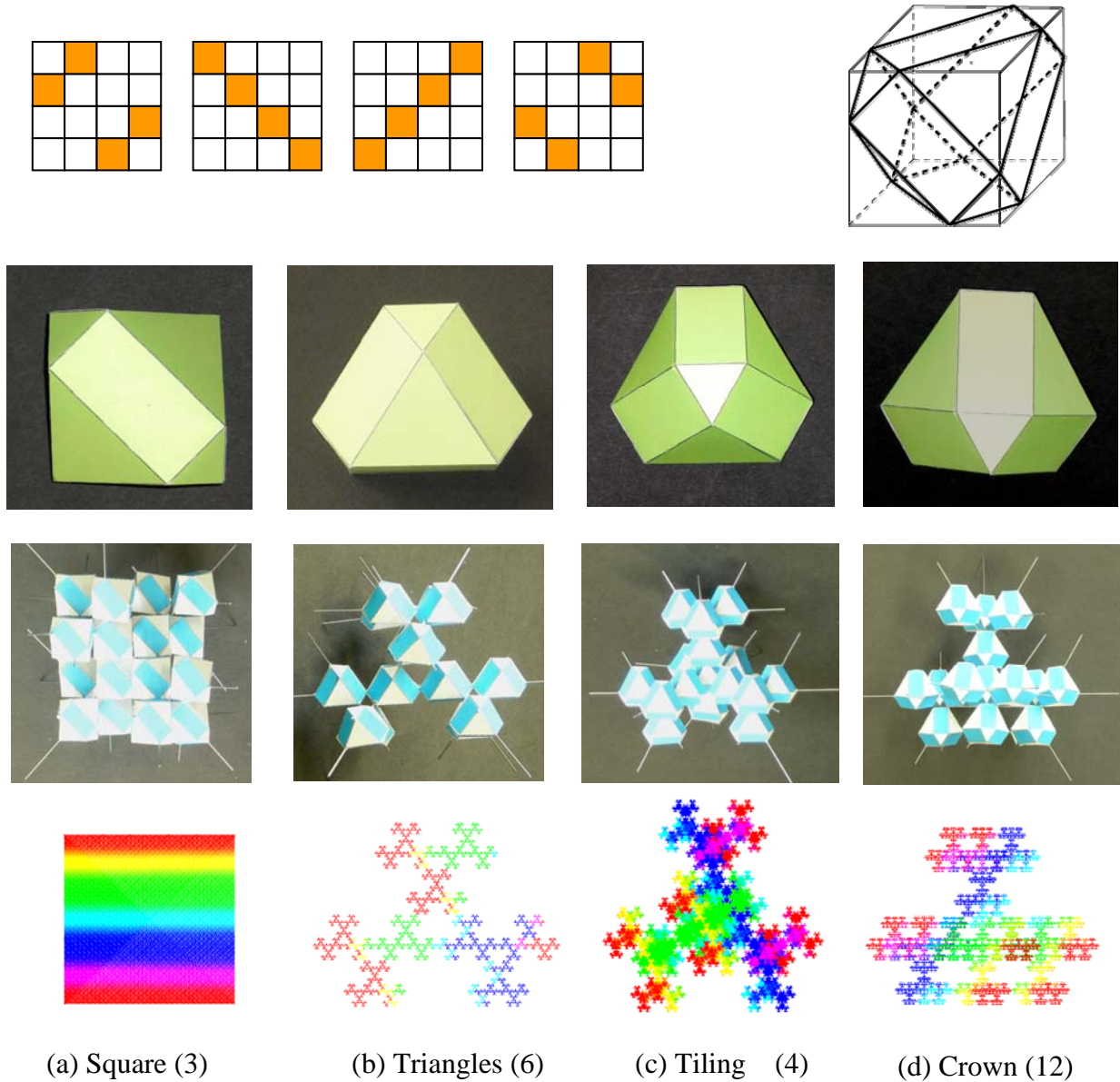


**Figure 8:** A series of configurations whose fractals converge to two sheets of triangles.



(a) Square (3)

(b) Triangles (6)

(c) Tiling (4)

(d) Crown (12)

**Figure 7:** *Non-Archimedean cuboctahedron fractal and its finite approximation models.*

Correspondingly, we have a sequence of fractals with three square projections. This sequence converges with respect to the Hausdorff metric and as the limit, we obtain a simple shape in Figure 9 which consists of two triangular sheets. Though this limit is not a self-similar fractal, when it is projected from three orthogonal directions, we have square images. In this figure, we have a simple application of this shape, which consists of two triangular sheets and three acrylic glass blocks which form a cube. On the two sheets, there are triangular drawings which form the triangular tiling of the plane, and one can see their affine-transformed connected images in three ways from three faces of the cube. There is another pair of tessellating drawings on the other sides of the sheets whose connected images can be seen from the other three faces.

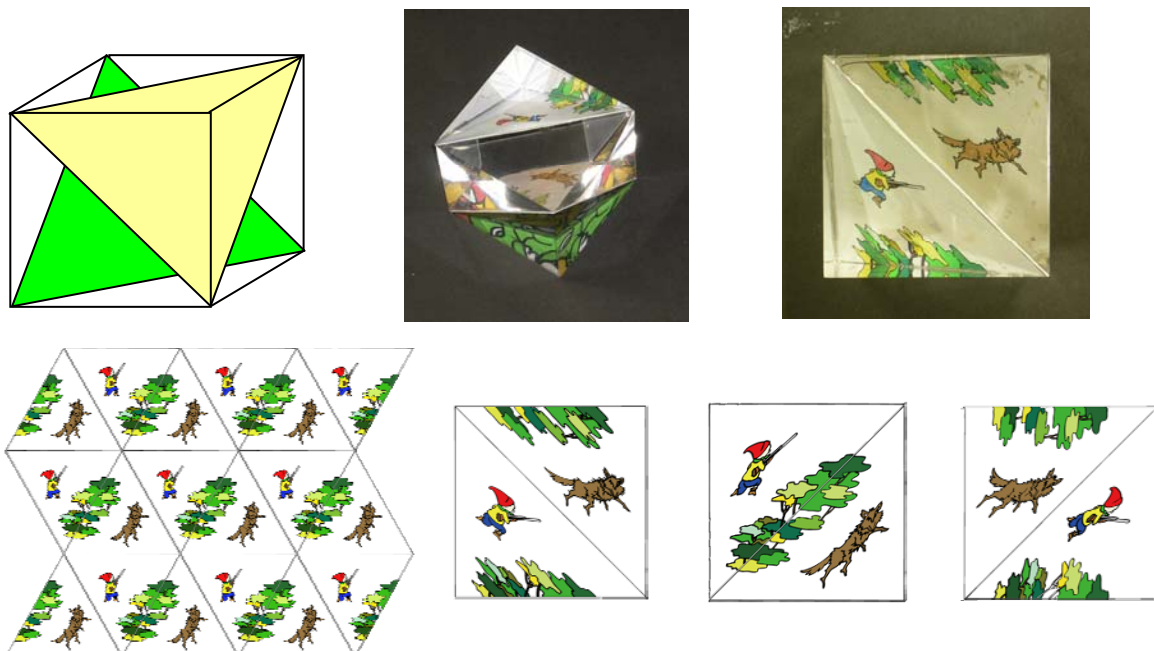


**Figure 9:** An object which displays three connected images of the triangular tessellation (acrylic glass, drawing by Yumiko Ihara).

### Tiling Patterns

We explain the tiling pattern Figure 10(c), which is a copy of Figure 5(d). It appears when the hexagonal bipyramid is projected from three pairs of vertexes of cubes containing it. Note that there are two cubes to consider and thus there are six such projections. As we have noted, it is also a self-similar figure and we study the similarity functions which form this figure. In Figure 10(a), the big hexagon is the projection image of this cube from an edge and the thick-lined hexagon is  $1/\sqrt{3}$  of the big hexagon rotated for 30 degree. One can see that the nine similarity functions of this figure map the thick-lined hexagon to the gray hexagons of size  $1/3$ . Note that the 9 gray hexagons are taken from the hexagonal tiling. Therefore, they are not overlapping and they in all have the same area as the thick-lined hexagon. In addition, this gray figure is a tiling pattern of the plane as (d) shows. Therefore, if we start with a hexagonal tiling and apply this procedure to all the tiles, we obtain a tiling with this gray figure. Since its repetition does not cause overlapping, we obtain a series of tiling patterns with the same area, whose limit is also a tiling pattern with the same area, which is Figure 10(c).

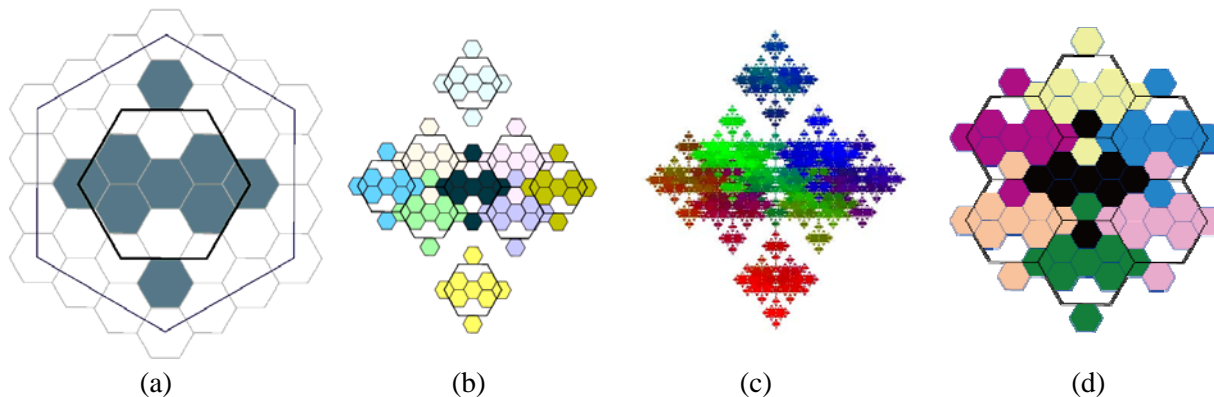


**Figure 10:** Tiling pattern of Figure 5(b).



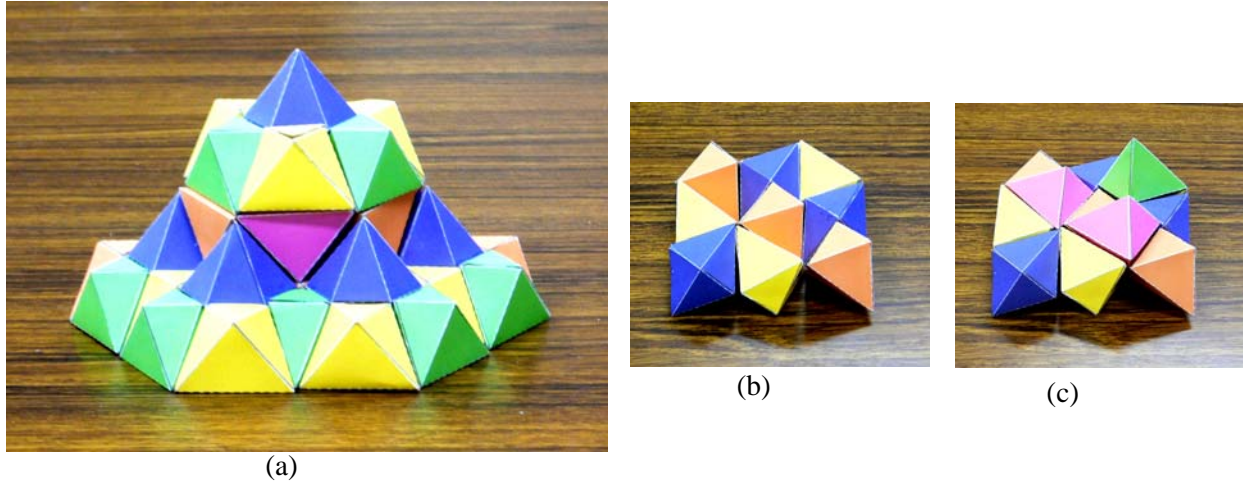


**Figure 11:** Tesselation with bipyramids and prismids. Bipyramids are blue(dark), and prismids have four bright colors.

tiling patterns Figure 1(c), 6(g), and 7(c) are obtained as vertex views of the surrounding cube, and have the same kind of explanation. Tiling patterns Figure 5(f) and 6(i) are projections from an edge of the cube, and they can also be understood in a similar way.

### A 3D Tiling with Hexagonal Bipyramids and Triangular Antiprismoids

Hexagonal bipyramids and triangular antiprismoids, which are the two kinds of polyhedra introduced as the convex hull of the fractals for the  $k=3$  case, have a strong connection. That is, there is a tiling of three-dimensional space with them as in Figure 11(a). The ratio of antiprismoids to bipyramids used for this tessellation is 4 to 1. In this picture, bipyramids have blue (dark) color, and antiprismoids are colored in four colors. In this section, we give mathematical backgrounds of this tiling.

We consider, in addition to the configurations in Figure 4, the following configuration which is the rotation of configuration G and thus also produces the antiprismoid fractal with a different orientation.

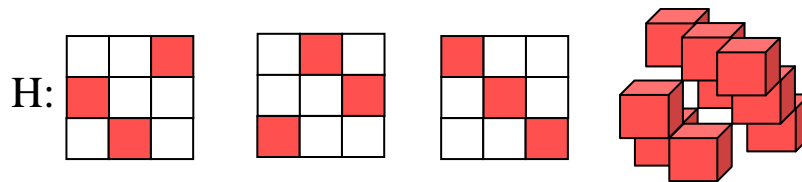


**Figure12:** Another configuration which generates the antiprismoid fractal.

Note that the three configurations F, G, and H are not overlapping. It means that the 1<sup>st</sup> level approximations of these three fractals are not overlapping. Therefore, we have  $3 \times 3 \times 3$  cubes which contain 9 bipyramids, 9 antiprismoids, and 9 antiprismoids with another orientation. Figure 11(b) is the picture of the lower level of this configuration. This configuration has 6 voids left around the corners of cubes. Note that polyhedra in adjoining cubes have the same polygon (or line) on their shared face. Therefore, each void is an octahedron surrounded by polyhedra in the surrounding 8 cubes. One can see that this octahedron is just an antiprismoid, because three of the vertices are located on corners of cubes and the other three are on middle points of edges of cubes. In Figure 11(c), three antiprismoids are placed in the three voids which exist between the lower and the middle level. Thus, we can fill the voids in the cube with six antiprismoids. This procedure can be generalized to the tiling of three-dimensional space

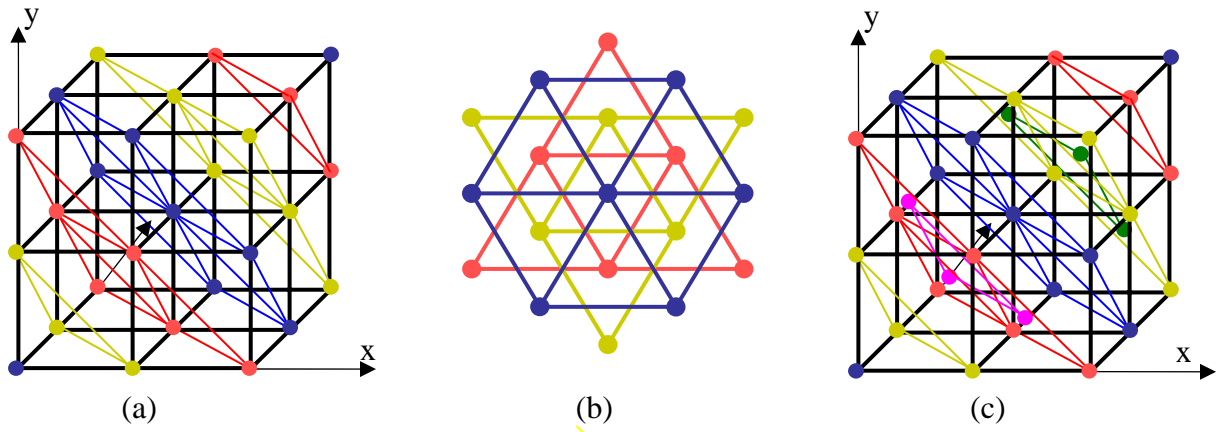


**Figure 13:** *The relation between a cubic 3D lattice(a), equilateral triangle lattices(b), and the points which generate the Voronoi tessellation(c).*

with cubes, and as the result, we obtain a tiling of the three-dimensional space with bipyramids and antiprismoids.

This tiling is the Voronoi tessellation in the following way. Let  $X$  be the cubic lattice of the centers of the cubes containing bipyramids and antiprismoids, described above. We define the center of a bipyramid (an antiprismoid) as the center of the cube containing it. We put the origin at the center of a bipyramid and give the coordinate system as in Figure 12(a).

Then, bipyramids are located on planes  $x + y + z = 3k$  for  $k$  integers, and antiprismoids coming from the configuration G and H are located on planes  $x + y + z = 3k+2$  and  $x + y + z = 3k + 1$ , respectively. On these three kinds of planes, points of the cubic lattice form equilateral triangle lattices. Figure 13(b) is parts of these lattices projected along the axis  $x = y = z$ . Let  $Y$  be the lattice obtained by rotating  $X$  around the axis  $x = y = z$  by 60 degree. The intersection of the two lattices  $X$  and  $Y$  is the union of the triangle lattices corresponding to  $x + y + z = 3k$  for  $k$  integers, that is, the centers of the bipyramids. Since our three-dimensional tiling has order 6 (60 degree) rotational symmetry around this axis, there are bipyramids and antiprismoids also on the lattice  $Y$ . Therefore, in this tiling, centers of the bipyramids are located on  $X \cap Y$  and the centers of antiprismoids are located on  $X \cup Y - X \cap Y$ , as in Figure 13(c). Note that the distance from the center of a bipyramid or an antiprismoid to faces with the same shape are the same, it is a Voronoi tessellation.

**Theorem:** The tiling with bipyramids and antiprismoids is the Voronoi tessellation corresponding to the union of a cubic lattice and its 60 degree rotation around a diagonal of one of the cubes.

#### Acknowledgements:

The author thanks Keiji Sugihara, Yohei Masuda, Yoshitaro Kurisu, and Tatsuki Nakajima for their help in assembling the models, and Yumiko Ihara for her drawing. He also thanks George Hart and Koji Miyazaki for their helpful comments on a draft version of this paper.

#### References:

- [1] Falconer, K.J. (1990) Fractal Geometry – Mathematical Foundations and Applications, John Wiley.
- [2] Barnsley, M.F.(1988) Fractals Everywhere, Academic Press.
- [3] Hideki Tsuiki, <http://www.i.h.kyoto-u.ac.jp/~tsuiki/index-e.html>.